

# Sorting and measurement of single gold nanoparticles in an optofluidic chip

Chen, Tian Ning; Liu, Ai Qun; Chin, Lip Ket; Wu, Jiu Hui; Shi, Yu Zhi; Sha, Xiong; Zhang, Yi

2017

Shi, Y. Z., Xiong, S., Zhang, Y., Chin, L. K., Wu, J. H., Chen, T. N., & Liu, A. Q. (2017). Sorting and measurement of single gold nanoparticles in an optofluidic chip. Proceedings of SPIE - Optical Trapping and Optical Micromanipulation XIV, 10347, 1034738-.  
doi:10.1117/12.2272114

<https://hdl.handle.net/10356/106363>

<https://doi.org/10.1117/12.2272114>

---

© 2017 SPIE. All rights reserved. This paper was published in Proceedings of SPIE - Optical Trapping and Optical Micromanipulation XIV and is made available with permission of SPIE.

*Downloaded on 28 Mar 2023 07:14:46 SGT*

# Sorting and measurement of single gold nanoparticles using an Optofluidic Chip

Y. Z. Shi<sup>a,b</sup>, S. Xiong<sup>a</sup>, Y. Zhang<sup>c</sup>, L. K. Chin<sup>a</sup>, J. H. Wu<sup>b</sup>, T. N. Chen<sup>b</sup>, A. Q. Liu<sup>\*a</sup>

<sup>a</sup>School of Electrical and Electronic Engineering, Nanyang Technological University, Singapore 639798; <sup>b</sup>School of Mechanical Engineering, Xi'an Jiao Tong University, Xi'an, 710049, China;

<sup>c</sup>School of Mechanical and Aerospace Engineering, Nanyang Technological University, Singapore 639798

\*Email address: eaqliu@ntu.edu.sg

## ABSTRACT

Gold nanoparticles have sparked strong interest owing to their unique optical and chemical properties. Their size-dependent refractive index and plasmon resonance are widely used for optical sorting, biomedicine and chemical sensing. However, there are only few examples of optical separation of different gold nanoparticles. Only separating 100–200 nm gold nanoparticles using wavelength selected resonance of the extinction spectrum has been demonstrated. This paper reports an optofluidic chip for sorting single gold nanoparticles using loosely overdamped optical potential wells, which are created by building optical and fluidic barriers. It is the first demonstration of sorting single nanoparticles with diameters ranging from 60 to 100 nm in a quasi-Bessel beam with an optical trapping stiffness from  $10^{-10}$  to  $10^{-9}$  N/m. The nanoparticles oscillate in the loosely overdamped potential wells with a displacement amplitude of 3–7  $\mu\text{m}$  in the microchannel. The sizes and refractive indices of the nanoparticles can be determined from their trapping positions using Drude and Mie theory, with a resolution of 0.35 nm/ $\mu\text{m}$  for the diameter, 0.0034/ $\mu\text{m}$  and 0.0017/ $\mu\text{m}$  for the real and imaginary parts of the refractive index, respectively. Here we experimentally demonstrate the sorting of bacteria and protozoa on the optofluidic chip. The chip has high potential for the sorting and characterization of nanoparticles in biomedical applications such as tumour targeting, drug delivery and intracellular imaging.

**Keywords:** Gold nanoparticle, optical sorting, Bessel beam, size and refractive index

## 1. INTRODUCTION

The optical trapping and manipulation has been successfully applied on the sub-nanoscale particles (e.g. atom  $\sim 10^{-10}$  m) based on an electric dipole moment in response to the electric field of light, and the microscale particles (e.g. cell  $\sim 10^{-5}$  m) based on the momentum transfer resulting from light scattering. However, it is difficult to apply these technologies for sorting and manipulating nanoparticles with the diameter of 1–100 nm. Because the optical force scales down approximately with the particle volume, thermal fluctuations are large enough to overwhelm the trapping forces at the nanoscale without cooling and vacuum environment. So far, only a few approaches have been developed to stably trap nanoparticles, including single beam, plasmonic resonance and optoelectronic tweezers [1–5].

Optical trapping has been used for the manual sorting of particles based on appearance or automated sorting based on their distinguished features such as size, shape and fluorescence. The focused laser beam is usually perpendicular to a fluid flow to selectively remove particles when the optical force is large enough to drive the particles out of the flow stream. An array of optical traps in the fluid flow can form an optical lattice to provide particle sorting. When a flow of mixed particles is passed through the lattice, selected particles are strongly deflected from their original trajectories, while others pass straight. Other interference patterns, either standing wave or fringe patterns can also successfully sort particles with the size varied from 300 nm to 10  $\mu\text{m}$ . However, the gradient force sorting methods in free space always suffer from diffraction limit and the dispersed energy by sub-patterns.

On the other hand, a low divergent beam propagates in the opposite direction of the fluid flow, in which the optical extinction force drives the particles move against the flow and optical gradient force draw them to the beam center. The particles are trapped when the optical force is equal to the drag force exerted on the particles. The trapping position is determined by the particle size, shape and refractive index etc. Stable trapping requires the axial gradient force to

dominate and is achieved when the beam diverges rapidly from the focal point, resulting in a high numerical aperture (N.A.) and small beam waist. To enable a slow beam divergence, this group of sorting uses a low N.A. ( $\sim 0.12$ ) Gaussian beam with large beam waist ( $10\text{--}20\ \mu\text{m}$ ), which gives rise to a shallow potential well with for nanoparticles smaller than  $100\ \text{nm}$  to escape easily [6–8].

In this paper, for the first time, an optofluidic chip is demonstrated for sorting gold nanoparticles with the diameter of  $60\text{--}100\ \text{nm}$  by using loosely overdamped optical potential wells with the optical trapping stiffness of  $10^{10}\text{--}10^9\ \text{N/m}$ . A quasi-Bessel beam is generated in the microchannel and propagates in the opposite direction of the flow stream. Potential wells are created by the barriers of optical force and drag force, which only have single equilibrium position for each gold nanoparticle in the microchannel. Oscillations of nanoparticles with the displacement of micrometers (i.e.  $4\text{ to }7\ \mu\text{m}$ ) triggered by the Brownian force are observed in those potential wells. On the other hand, the refractive indices and sizes of the nanoparticles are determined through the trapping process in the optofluidic chip. In addition, sorting of the bacteria and protozoa is achieved by using this optofluidic chip.

## 2. THEORETICAL ANALYSIS

Figure 1a shows the schematics of the optofluidic chip, which consists of a microfluidic and an optical part. The microfluidic part includes a microchannel, three inlets and two outlets. Deionized water is pumped from the two side-inlets to form sheath flow streams. Gold nanoparticles are injected from the central inlet to the outlet, and confined in the middle of the microchannel by the hydrodynamic focusing. The optical part includes a micro-quadrangular lens and a laser source. A quasi-Bessel beam is realized by irradiating a fiber laser ( $\text{NA} = 0.12$ ) through the micro-quadrangular lens, which is coupled into the flow stream along the microchannel from outlet to inlet. The beam has a tight focusing main lobe (minimum  $0.9\ \mu\text{m}$ ) and diverges slowly with an equivalent NA smaller than  $0.05$  in a propagating length over

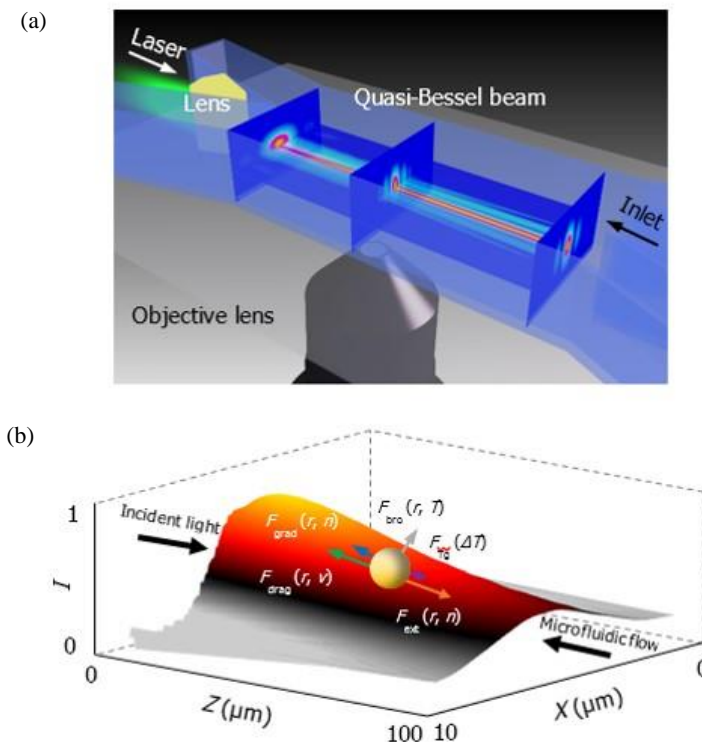


Figure 1. Design of the nanoparticle trapping in an optofluidic chip. (a) Schematic illustration of the optofluidic chip. (b) Force analysis of the gold nanoparticle in the microchannel.

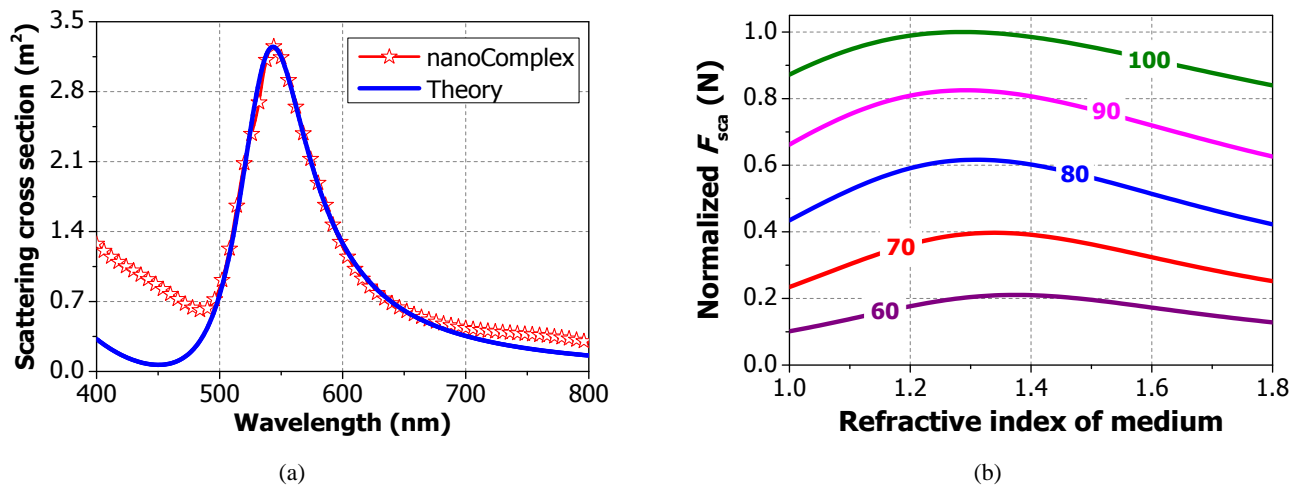


Figure 2. Theoretical analysis of the optical forces. (a) Calculated and measured optical scattering cross section with wavelength. (b) Normalized optical scattering force on particles with different sizes versus the refractive index of the medium.

100  $\mu\text{m}$ , as shown in Fig. 1b. Thus, it exerts a dominating optical extinction force ( $F_{\text{ext}}$ ) and weak optical gradient force ( $F_{\text{grad}}$ ) on the nanoparticle along the light propagation direction. Meanwhile, the nanoparticle is affected by the drag force ( $F_{\text{drag}}$ ) along the flow stream direction. The dramatic heating by the laser causes distinctly temperature increase on the nanoparticle, which makes the Brownian force ( $F_{\text{bro}}$ ) play an important role in the nanoparticle dynamics. Due to the interaction of the absorption of the laser energy and the dissipation of heat to the ambient flow stream, temperature distribution along the microchannel is not uniform, resulting in a temperature gradient force ( $F_{\text{Tg}}$ ). The equilibrium of the forces makes the nanoparticle trapped in the microchannel.

The refractive indices of gold nanoparticles can be obtained by fitting the optical scattering spectrum. Figure 2 presents the calculated and measured optical scattering cross section with wavelength. The theory used to calculate the optical scattering cross section is modified from Drude theory by adding a proportional factor. The calculation fits well with the measurement when the wavelength is above 500 nm. Figure 3 shows the normalized optical scattering force on different nanoparticles with different sizes when the refractive index of the medium is changed. When the light intensity of the quasi-Bessel beam is sufficiently strong to generate air bubble on the gold nanoparticles, the refractive index of the surrounding medium changes. As a result, the optical force changes.

### 3. EXPERIMENTAL RESULTS AND DISCUSSIONS

When the nanoparticles flow into this optical field, the nanoparticles with different sizes are trapped at different positions as shown in Fig. 3a. The power used in this experiment is 400 mW and the flow rate is 300  $\mu\text{m s}^{-1}$ . The different diameters of nanoparticles from 60, 70, 80, 90 to 100 nm are trapped in the different position along the microchannel, i.e.  $z = 32.5, 74.7, 104.6, 113.1$  and 132  $\mu\text{m}$ , respectively. Their trapping positions are also separated and marked by the white dash line in Fig. 3a. The force analysis reveals that the optical extinction force and drag force play the dominant roles in the trapping. Larger nanoparticles are trapped far from the lens ( $z = 0$ ) because of the larger optical extinction forces acting on them. These experimental data can be used to calibrate the functions between the trapping positions and diameters of the nanoparticle. When a nanoparticle is trapped in the optofluidic field, its diameter can be measured based on its trapping position. Meanwhile, its refractive index is calculated accordingly. When the diameter of the nanoparticle increases from 60 to 100 nm, the real part of the refractive index increases from 0.6704 to 1.1527, while the imaginary part of RI decreases from 2.0024 to 1.8171. The long trapping range (32–132  $\mu\text{m}$ ) of the nanoparticles enables a high resolution of diameter, real and imaginary parts of the refractive index with 0.35 nm/ $\mu\text{m}$ , 0.0034/ $\mu\text{m}$  and 0.0017/ $\mu\text{m}$ , respectively.

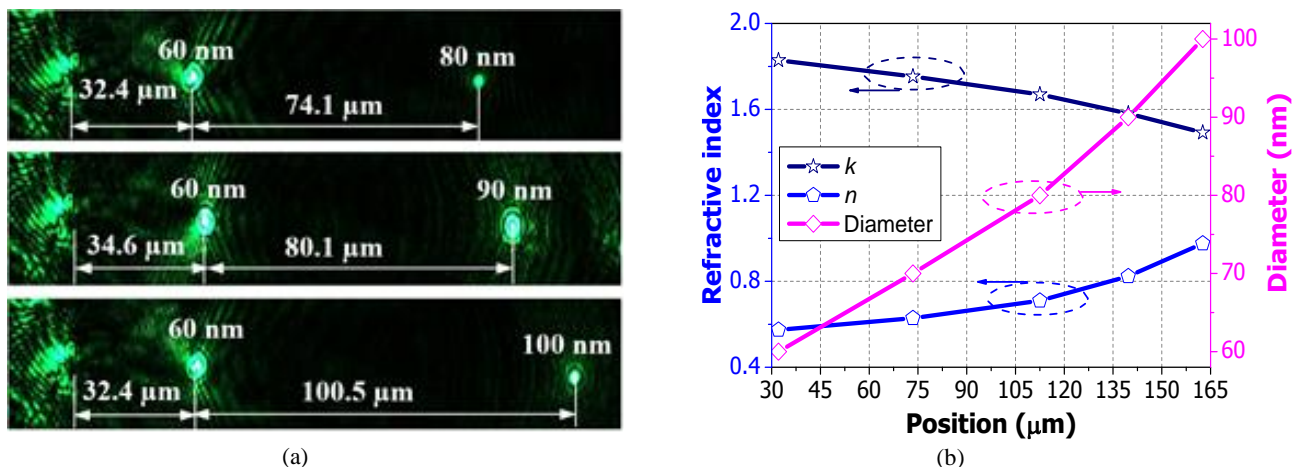


Figure 3. (a) Experimental observation of sorting of nanoparticles along the microchannel. (b) Measurement of the size and refractive indices of gold nanoparticles.

#### 4. CONCLUSIONS

In conclusion, for the first time, gold nanoparticles with the diameters ranging from 60 to 100 nm are sorted by creating isolated optical potential wells in an optofluidic chip. The potential wells are realized by combining the optical and fluidic forces, and trap the nanoparticles at any position by tuning the laser intensity and flow rate. Oscillations of nanoparticles with large displacements ( $4 \sim 7 \mu\text{m}$ ) are observed in the loosely overdamped optical potential wells with the trapping stiffness of  $10^{-10}$ – $10^{-9}$  N/m, which is much larger than that in the tightly focused optical tweezers. Since one nanoparticle can only be trapped in a certain position along the microchannel, the refractive index and size of the nanoparticle can be determined by its trapping position. It enables a high resolution of diameter, real and imaginary parts of the refractive index with  $0.35 \text{ nm}/\mu\text{m}$ ,  $0.0034/\mu\text{m}$  and  $0.0017/\mu\text{m}$ , respectively. The optofluidic chip provides a promising technology for various biomedical applications such as tumor targeting, DNA and drug delivery and intracellular biochemical composition imaging, which requires a high degree of accuracy on the size selective control and manipulation of nanoparticles in solution.

#### ACKNOWLEDGEMENTS

This work was supported by Singapore National Research Foundation under the Competitive Research Program (NRF-CRP13-2014-01), and under the Incentive for Research & Innovation Scheme (1102-IRIS-05-02) administered by PUB.

#### REFERENCES

- [1] Yang, Y., Liu, A. Q., Chin, L. K., Zhang, X. M., Tsai, D. P., Lin, C. L., Lu, C., Wang, G. P. and Zheludev, N. I., "Optofluidic waveguide as a transformation optics device for manipulation," *Nat. Commun.* 3, 651 (2012).
- [2] Xiong, S., Liu, A. Q., Chin, L. K. and Yang, Y., "An optofluidic prism tuned by two laminar flows," *Lab Chip* 11, 1684–1869 (2011).
- [3] Yang, Y., Liu, A. Q., Lei, L., Chin, L. K., Ohl, C. D., Wang, Q. J. and Yoon, H. S., "A tunable 3D optofluidic waveguide dye laser via two centrifugal Dean flow streams," *Lab Chip* 11, 3182–3187 (2011).

- [4] Zhao, H. T., Yang, Y., Chin, L. K., Chen, H. F., Zhu, W. M., Zhang, J. B., Yap, P. H., Liedberg, B., Wang, K., Wang, G., Ser, W. and Liu, A. Q., "Optofluidic Lens with Low Spherical and Low Field Curvature Aberrations," *Lab on a Chip*, 16, 1617–1624 (2016).
- [5] Shi, Y. Z., Xiong, S., Chin, L. K., Yang, Y., Zhang, J. B., Ser, W., Wu, J. H., Chen, T. N., Yang, Z. C., Hao, Y. L., Liedberg, B., Yap, P. H., Zhang, Y. and Liu, A. Q., "High-resolution and multi-range particle separation by microscopic vibration in an optofluidic chip," *Lab on a Chip*, (2017).
- [6] Li, Z. G., Xiong, S., Chin, L. K., Ando, K., Zhang, J. B. and Liu, A. Q., "Water's tensile strength measured using an optofluidic chip," *Lab on a chip*, 15, 2158–2161 (2015).
- [7] Xiong, S., Chin, L. K., Ando, K., Tandiono, T., Liu, A. Q. and Ohl, C. D., "Droplet generation via a single bubble transformation in a nanofluidic channel," *Lab Chip*, 15, 1451–1457 (2015).
- [8] Li, Z. G., Liu, A. Q., Klaseboer, E., Zhang, J. B. and Ohl, C. D., "Single cell membrane poration by bubble-induced microjets in a microfluidic chip," *Lab Chip*, 13, 1144–1150, (2013).